

Optical studies of electron and hole Fermi seas in a single GaAs/Al_xGa_{1-x}As quantum well

S. R. Andrews

*GEC Research Ltd., The General Electric Co., p.l.c., Hirst Research Centre,
East Lane, Wembley, Middlesex HA9 7PP, United Kingdom*

A. S. Plaut*

The Clarendon Laboratory, University of Oxford, Parks Road, Oxford OX1 3PU, United Kingdom

R. T. Harley†

*GEC Research Ltd., The General Electric Co., p.l.c., Hirst Research Centre,
East Lane, Wembley, Middlesex HA9 7PP, United Kingdom
and The Clarendon Laboratory, University of Oxford, Parks Road, Oxford OX1 3PU, United Kingdom*

T. M. Kerr

*GEC Research Ltd., The General Electric Co., p.l.c., Hirst Research Centre,
East Lane, Wembley, Middlesex HA9 7PP, United Kingdom
and The Clarendon Laboratory, University of Oxford, Parks Road, Oxford OX1 3PU, United Kingdom*

(Received 18 September 1989)

The optical properties of a sample containing several GaAs quantum wells of different widths separated by relatively thick but leaky Al_{0.3}Ga_{0.7}As barriers are investigated at temperatures up to 150 K. Electrical bias, applied using a Schottky gate, tilts the energy bands and results in quiresonant transfer of electrons or holes, photoexcited in thicker GaAs layers into the quantum wells. This permits investigations under conditions varying from no significant carrier population up to electron or heavy-hole sheet densities of about $2 \times 10^{11} \text{ cm}^{-2}$ in the same quantum well and provides detailed information on the formation of "Mahan excitons," oscillator strengths, and band-gap renormalization.

I. INTRODUCTION

The band-edge optical properties of semiconductor quantum wells are strongly affected by the existence of excitons. In addition to intrinsic wells, interest has recently turned also to understanding the optical effects of free carriers, particularly in the one-component Coulomb systems which can be created using modulation doping. In these structures the carriers are spatially separated from the dopants so that ionized-impurity scattering is reduced and high-mobility quasi-two-dimensional (quasi-2D) Fermi gases can be created. They demonstrate interesting many-body effects in the optical properties not easily seen in doped bulk semiconductors.¹⁻³ In particular, the collective behavior of the Fermi sea in the process of creation or annihilation of an electron-hole pair is important.

At low temperatures and carrier concentrations the dielectric response of a quantum well at energies near the direct band gap is dominated by atomic exciton states. With increasing doping, carrier-carrier interactions in the form of many-body exchange and correlation effects cause a renormalization of the single-particle energies. This can be approximately described as a rigid shift of the conduction and valence subbands towards each other and affects all subbands in a similar way.^{3,4} If both subbands involved in the optical transition are unoccupied, then the atomic exciton remains well defined up to carrier sheet densities of $\sim 10^{12} \text{ cm}^{-2}$,⁵ which is larger than in

the case of bulk material. This is because in two dimensions, screening of the long-range Coulomb interaction is weaker than in three dimensions and, at low temperatures, saturates at large carrier densities because of the constant density of states.^{6,7} If one of the subbands is occupied, then the exclusion principle, in the form of phase-space filling and short-range exchange interactions between carriers in the Fermi sea, leads to quenching of the atomic exciton. At low temperatures the limit of stability is the Mott density, given by $k_F a_0 \sim 1$, where k_F is the wave vector at the Fermi surface and a_0 is the Bohr radius of the atomic exciton.⁸ Beyond this limit the renormalized band gap falls below the exciton energy, or equivalently, the exciton binding energy becomes less than the combined Fermi level. Typically this corresponds to a carrier density of a few times 10^{11} cm^{-2} .

Although for quite low sheet carrier densities the atomic exciton unbinds, when allowance is made for the dynamical response of the Fermi sea in the case of a degenerate electron gas, final-state interactions of the electron and hole have a pronounced effect on the absorption spectrum in three dimensions⁹ and an even larger effect in two dimensions.¹⁰ At low temperatures these effects manifest themselves in the appearance of an excitonlike peak, the "Mahan exciton,"⁹ which is a bound state with respect to the Fermi level. Physically, the oscillator strength at the Fermi edge is enhanced because the many-body correlation of the photoexcited minority carrier with the majority-carrier Fermi sea increases the

electron-hole overlap relative to the statically screened case.^{9,10} The enhancement is strongest at the Fermi edge because, below E_F , electron-hole multiple scattering is suppressed by phase-space blocking. It has been remarked that this phenomenon is analogous to the Fermi-edge singularity in the x-ray absorption and -emission spectra of metals,^{11,12} although in the semiconductor case the singularity is smeared out by hole-recoil effects. In general, the recombination for both low and high concentrations of a single carrier type is expected to be a wave-vector-conserving process and therefore to show a peak at the fundamental gap.^{1,13} However, hole localization in alloy systems may relax this selection rule giving an additional peak at the Fermi energy.¹⁴

Ideally, one would like to vary the carrier density in a continuous manner in order to make systematic studies of the many-body effects. One approach is to use a modulation-doped quantum well as the channel of a field-effect transistor and so vary the electron or hole concentration with the gate voltage. However, this only makes possible the control of one type of carrier, according to whether the modulation doping is p or n type. In this paper we describe experiments on a structure in which it is possible to change the carrier type, as well as to vary their densities from essentially zero up to $2 \times 10^{11} \text{ cm}^{-2}$. It is grown on a conducting substrate, but is otherwise undoped, and therefore retains the advantage of spatial separation of carriers from impurities.

To investigate the optical properties of this structure, we have used a variety of techniques. Here we describe photoluminescence (PL) and photoluminescence excitation (PLE) measurements at temperatures up to 150 K, which establish the details of the charge accumulation in the wells at different applied bias. They also reveal the formation of "Mahan excitons" at the Fermi level (or, more generally, at the quasichemical potential), and the changes in oscillator strengths and band-gap renormalization when electron or hole Fermi seas are present in the wells, and their temperature dependence. We have also made studies of effects of carriers on magneto-PL (Ref. 15) and on exciton dephasing by means of resonant Rayleigh scattering, which will be described elsewhere.¹⁶

II. EXPERIMENT

The sample (see Fig. 1) consisted of intrinsic GaAs wells of thickness 5, 10, 20, and 80 nm separated by 34-nm $\text{Al}_{0.3}\text{Ga}_{0.7}\text{As}$ barriers grown by molecular-beam epitaxy (MBE), on an n^+ -type GaAs substrate with an intervening 0.5- μm -thick undoped GaAs buffer layer. The layer thicknesses were measured by transmission electron microscopy (TEM). A background p -type doping of $\sim 3 \times 10^{14} \text{ cm}^{-3}$ (probably carbon acceptors) was found in GaAs epilayers grown immediately after the above structure, and residual p -type doping in the $\text{Al}_x\text{Ga}_{1-x}\text{As}$ layers is probably somewhat higher. Electric fields were applied perpendicular to the layers using a 100-nm-thick, 90% transparent indium tin oxide (ITO) Schottky contact on the top surface and an Ohmic indium alloy con-

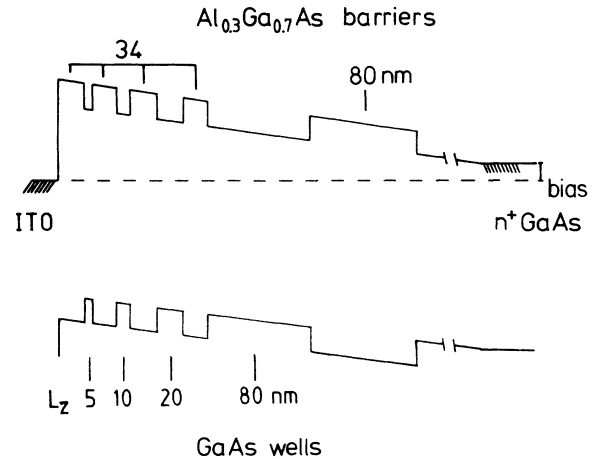


FIG. 1. Schematic of the sample structure.

tact on the substrate. The zero-electric-field or flat-band condition was identified as $0.35 \pm 0.05 \text{ V}$ applied bias from the null point of the photocurrent in the sample. This is also approximately the saturation voltage obtained with intense illumination at energies above the $\text{Al}_x\text{Ga}_{1-x}\text{As}$ band gap.

Closely similar electrical behavior and spectra were observed using a 20% transmitting layer of gold in place of the ITO. The ITO acts as an antireflection coating, so that the luminescence intensities are roughly twice that of the uncoated material and about 50 times that obtained with the gold electrode. This allowed measurements over a considerable range of incident power densities, the results discussed here being for $\sim 0.1 \text{ W cm}^{-2}$, well below that required to produce saturation or carrier-heating effects. Most of the data in this paper refer to the 5-nm well, but qualitatively similar results were obtained for the 10- and 20-nm wells. The sample was mounted in a strain-free manner in a helium atmosphere in a variable-temperature cryostat.

Our optical equipment consisted of an argon-ion-pumped Styryl-9 or Pyridine-2 dye laser to excite the sample. It was tuned with a birefringent filter giving a linewidth [full width at half maximum (FWHM)] of $\sim 0.1 \text{ meV}$. Light from the sample was analyzed using a 0.85-m-focal-length double-grating spectrometer, also with a resolution of $\sim 0.1 \text{ meV}$, and was detected using a cooled GaAs photomultiplier with photon-counting electronics.

Measurements were made with the dye laser incident at an angle of $\sim 15^\circ$ to the surface normal of the sample, focused to a spot $\sim 50 \mu\text{m}$ in diameter and polarized with its E vector in the plane of the surface. Light was collected at $\sim 90^\circ$ to the incident beam with $f/1.8$ optics. PL was examined by using a fixed dye-laser energy well above the absorption edge and scanning the spectrometer through the region of interest. PLE spectra were obtained by setting the spectrometer to detect near the maximum of the first conduction subband to first heavy-hole subband ($E1-H1$) recombination peak and scanning the dye laser to higher energy.

III. EFFECTS OF CARRIERS AT LOW TEMPERATURES

Examples of PL and PLE spectra at 5 K for the 5-nm well at different applied biases are shown in Fig. 2. At this low temperature the PL spectrum in each case consists of a single line due to the intrinsic $E1-H1$ recombination, first conduction subband to first light-hole subband ($E1-L1$) recombination being negligibly weak. The PLE spectra contain two peaks, that at lower energy associated with $E1-H1$ absorption and that at higher energy with $E1-L1$ absorption. In our treatment of the PLE data we have assumed that the luminescence intensity is directly proportional to absorption and that the continuum absorption well above the $E1-L1$ transition is approximately independent of bias and carrier density. The latter assumption is based on consideration of oscillator-strength sum rules¹⁷ and allows us to scale the spectra obtained at different biases relative to that at flat band (0.35 V).

There are several significant changes in the spectra

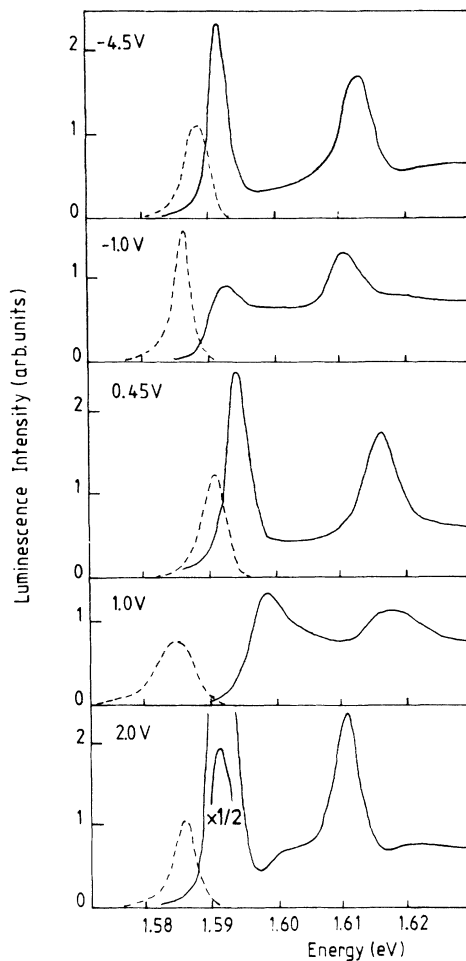


FIG. 2. Photoluminescence excitation (PLE) (solid curves) and photoluminescence (dashed curve) spectra at 5 K for the 5-nm well at different biases. The intensity of the PLE spectra are scaled relative to one another as described in the text.

with increasing forward and reverse bias, which can be understood in terms of creation of Fermi seas of electrons or heavy holes in the wells due to quasiresonant carrier injection. Firstly, the energy difference ("Stokes shift") between the emission- and absorption-peak positions changes markedly; a detailed plot is shown in Fig. 3. Secondly, there is a shift of the PL-peak position, as shown in detail in Fig. 4. Thirdly, at biases corresponding to the maxima of the "Stokes shift," there is a broadening and reduction in the integrated area under the $E1-H1$ exciton peaks in the PLE spectra, relative to that of the continuum at higher energy, which indicates a decrease in oscillator strength by a factor of order 2–3. These effects can be seen by comparing the spectra at ± 1.0 V with that at 0.45 V in Fig. 2.

In interpreting the "Stokes-shift" data (Fig. 3), we assume that the relatively small shift of ~ 3 meV under flat-band conditions has its origin in efficient trapping of the delocalized excitons at regions, perhaps of order of a few tens of nm in extent, where the well is 1 or 2 monolayers wider than average. The increased values of the "Stokes shift" for biases away from flat band indicate an additional contribution due to the Moss-Burstein shift¹⁸ associated with Fermi seas of electrons and heavy holes. We expect that, in this case where the wells are GaAs, wave vector will be conserved in the absorption and recombination processes.^{1,13} This is in contrast to the situation for alloy wells, where carrier localization can be dominant.¹⁴ Thus the recombination occurs predominantly at $k=0$, whereas absorption occurs at a higher energy between valence- and conduction-band states at

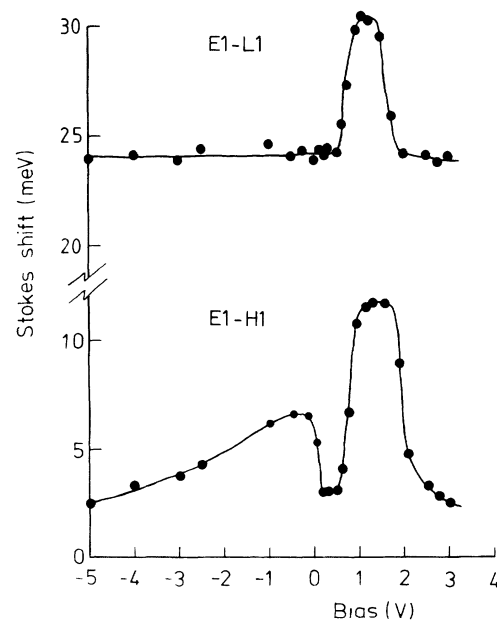


FIG. 3. Bias dependence of the "Stokes shift" between the $E1-H1$ transition in emission and the $E1-H1$ and $E1-L1$ transitions in absorption for the 5-nm well at 5 K as deduced from photoluminescence excitation spectra.

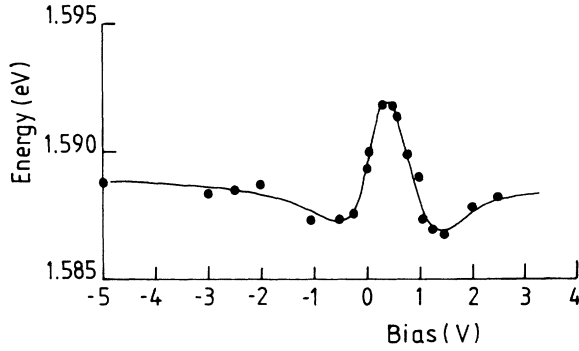


FIG. 4. Variation of photoluminescence peak energy as a function of bias for the 5-nm well at 5 K.

the Fermi wave vector k_F (see Fig. 5). Under these conditions, band-gap renormalization and changes in the exciton energy due to space charge as well as effects of band bending and electric field on the energy levels make no net contributions to the “Stokes shift” of the heavy-hole “exciton” peak since they contribute equally to the absorption and emission energies. The “Stokes shift” of the “heavy-hole” peak may then be used to obtain a value of the Fermi energy and carrier concentration in the well. It is clear from Figs. 2 and 3 that the additional “Stokes shifts” for positive bias between 0.60 and 2.0 V is due to the presence of a Fermi sea of electrons, since both the heavy- and light-hole transitions show a similar shift and loss of integrated intensity. However, for biases between 0 and -4 V the light-hole transition shows no significant shift and little broadening (<0.5 meV), indicating that under these conditions there is a Fermi sea of heavy holes present, the light-hole band being empty. There is a

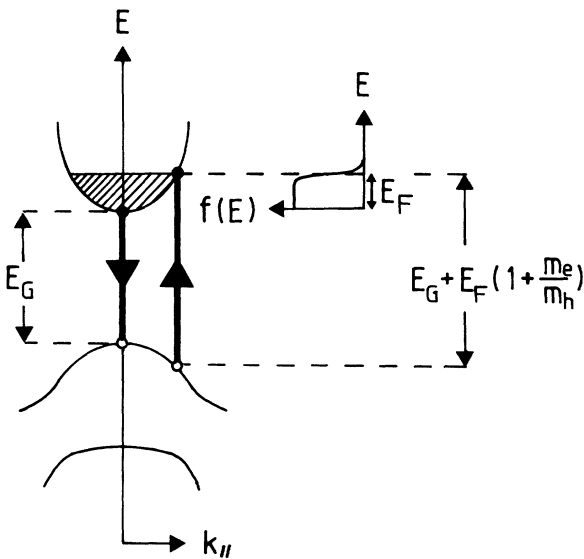


FIG. 5. Schematic of absorption and emission processes with an occupied conduction subband.

small decrease in oscillator strength relative to the continuum background that we tentatively attribute to band mixing. We shall discuss in Sec. V the mechanism for accumulation of electrons or holes in this structure.

The sheet carrier densities N_s are obtained from the “Stokes shift” (Fig. 3) as follows. We assume a two-dimensional density of states with parabolic electron and hole dispersion and also assume that optical transitions conserve wave vector ($\Delta k = 0$). The extra “Stokes shift” is given by

$$\Delta E = \frac{\pi \hbar^2}{m_{\text{ex}}} N_s = \frac{\hbar^2 k_F^2}{2m_{\text{ex}}},$$

where $m_{\text{ex}}^{-1} = m_e^{-1} + m_h^{-1}$, and m_e and m_h are the effective masses of the electron and hole, respectively.

We use the value of $m_{\text{ex}}/m_0 = 0.050$ obtained for undoped 5-nm wells in recent low-field magnetorefectivity experiments.¹⁹ From the observed extra “Stokes shift” of 8.6 meV, the peak N_s is $1.8 \times 10^{11} \text{ cm}^{-2}$ for electrons in forward bias with $E_F = 6.3$ meV and $k_F a_0 = 1.05$. Similarly, with a maximum extra “Stokes shift” of 3.6 meV in reverse bias, and heavy-hole density is $0.75 \times 10^{11} \text{ cm}^{-2}$, $E_F = 1.0$ meV, and $k_F a_0 = 0.69$. It is difficult to estimate the carrier type and density under flat-band conditions, but if limited by residual p -type doping, then it is probably less than 10^9 cm^{-2} .

We estimated the photoexcited carrier densities in these measurements to be 10^8 cm^{-2} , $\sim 10^{-3}$ of the maximum sheet densities calculated above. This estimate is based on a recombination time of 300 ps,²⁰ an absorption coefficient of 10^4 cm^{-1} , and cw pumping power of 0.1 W cm^{-2} . We observed no change in peak charge densities for intensities between 10^{-3} and 10 W cm^{-2} .

The effect of the space charge and electric field on the single-particle energies can be estimated using the variation of the $E1$ - $H1$ luminescence-peak position, Fig. 4, and from knowledge of the changes in exciton binding energy. As discussed in Sec. I, the atomic exciton binding energy is predicted to become very small for quite modest carrier densities,²¹ while the optical strength remains observable. Similarly, the binding energy of the 2D “Mahan exciton,” although enhanced over the 3D case,^{9,22} will probably be less than 1 meV. Indeed, we have verified from magneto-PL measurements, described elsewhere,¹⁵ that the exciton binding energy at flat band in the 5-nm well is approximately 10 meV and becomes very small with increasing carrier density. The combined renormalization, due to an electric field of order $5 \times 10^4 \text{ V cm}^{-1}$ and the space charge, is 15.0 meV for $1.8 \times 10^{11} \text{ cm}^{-2}$ electrons and 14.6 meV for $0.75 \times 10^{11} \text{ cm}^{-2}$ holes. We estimate the change in Hartree energies due to electric field and the band-bending effects of space charge to be ~ 3.2 meV, leaving 11.8 and 11.4 meV as the band-gap renormalization associated with the electron and heavy-hole populations, respectively. The main uncertainty in these values lies in the assumption of uniform potential drop across the structure.

A rough estimate of the order-of-magnitude error involved can be made by assuming that only the 5-nm well is occupied with sheet charge density σ . The electric

field experienced by the well will be different from the unoccupied case by an amount of order σ/ϵ , where ϵ is the dielectric constant. This leads to changes in the computed Stark shift, and therefore also in the band-gap renormalization, of about 1 meV.

Schmitt-Rink and Eli⁷ give an expression for the band-gap renormalization in two dimensions,

$$\delta E_{2D} = -3.1 \left[\frac{N_s a_0^2}{2} \right]^{1/3} E_{1s},$$

where E_{1s} is the exciton binding energy. Using the effective parameters appropriate to the 5-nm well ($a_0 = 10$ nm and $E_{1s} = 10$ meV rather than the theoretical 2D values), we find $\delta E = 13.9$ meV in forward bias and 10.4 meV in reverse bias, values close to our measurements and consistent with calculations for finite well width by Kleinman and Miller.⁴ Note that our data show a significantly larger band-gap renormalization (by about 30%) for a hole sea than for an electron sea of the same density. A similar but smaller effect was calculated by Kleinman and Miller.⁴

The observed dependence of the linewidth and oscillator strength of the excitonic peaks upon carrier concentration are discussed more fully in Sec. V.

IV. CIRCULARLY POLARIZED PHOTOLUMINESCENCE EXCITATION

In their circularly polarized PLE experiments, Ruckenstein *et al.*² observed a reversal of circular polarization of the $n = 2$ transition in an n -type-doped quantum well

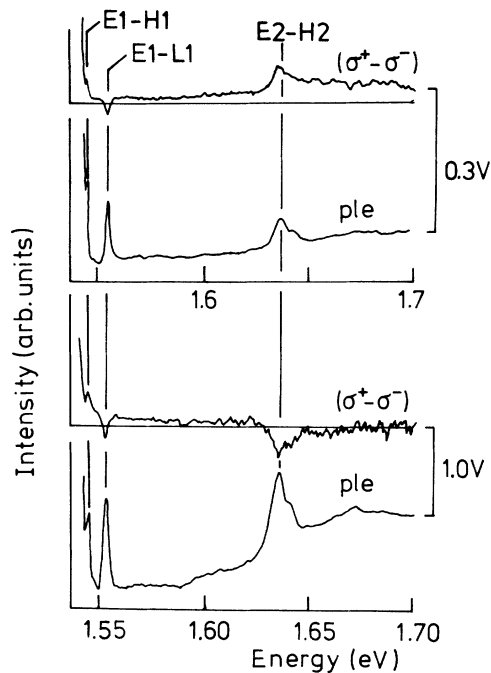


FIG. 6. Circularly polarized and unpolarized photoluminescence excitation spectra for the 10-nm well (a) at flat band (0.3 V) and (b) with $\sim 10^{11}$ electrons cm^{-2} present (1.0 V).

compared to that observed in an undoped well. We have not studied this phenomenon in any detail, but have used the polarization of the $n = 2$ exciton peak as a monitor of the presence or absence of an electron Fermi sea. Our polarized PLE spectra were obtained from the 10-nm well (where a significant electron population is present for biases between 0.5 and 1.0 V and a hole population between 0.1 and -0.5 V). We used circularly polarized excitation and measured the circular polarization of the luminescence ($I_{\sigma^+} - I_{\sigma^-}$) with a differential ratemeter while simultaneously recording the unpolarized PLE spectra. With flat bands, Fig. 6(a), the excitation spectrum shows the $n = 1$ and heavy-hole and the $n = 1$ light-hole transitions. The corresponding polarization spectrum is as expected, with positive peaks for the heavy-hole transitions and a lower or even negative polarization for the light-hole transition. However, at a bias of 1.0 V, even though the PLE spectrum near the $n = 2$ transition does not appear particularly changed, Fig. 6(b), the polarized PLE spectrum exhibits a reversal in the sign of the $n = 2$ polarization, which is consistent with a Fermi sea of electrons being present. No change is observed in the polarization spectrum when a Fermi sea of holes is present, in agreement with Ruckenstein *et al.*²

V. TEMPERATURE-DEPENDENT EFFECTS

The effect of increasing temperature on the PL and PLE spectra of the 5-nm well is illustrated for various applied biases in Fig. 7, which shows “Stokes shift” and linewidth for the $E1-H1$ transition. The behavior is very different depending on the presence or absence of carriers. With no significant carriers in the well (0.30 V), the linewidth [Fig. 7(a)] is approximately 4 meV at low temperatures and shows a linear increase with temperature. This is consistent with a dominant temperature-independent inhomogeneous component superimposed on broadening due to acoustic-phonon scattering, which is expected to be $\sim 10 \mu\text{eV}/\text{K}$.²³ LO-phonon scattering will not be important over this temperature range. At the same time, the “Stokes shift” [Fig. 7(b)] falls sharply as excitons are thermally activated out of the few-meV-deep potential wells formed by layer-thickness fluctuations. The oscillator strength of the PLE peak varies only weakly with temperature.

The behavior as temperature is increased with Fermi seas of carriers in the wells is markedly different. The “Stokes shift” for both electrons (1.50 V bias, $N_s \approx 1.8 \times 10^{11} \text{ cm}^{-2}$, and $E_F \approx 6.3$ meV) and holes (-0.70 V bias, $N_s \approx 0.75 \times 10^{11} \text{ cm}^{-2}$, and $E_F \approx 1.0$ meV) shows a rapid initial decrease, corresponding with that for the empty well, superimposed on a more gradual reduction towards zero at ~ 100 K. The linewidths [Fig. 7(a)] are difficult to measure quantitatively due to the asymmetry of the spectra (Fig. 2), but, at low temperatures, are increased by a few meV compared to the empty well, partly resulting from hole-recoil effects of order $2E_F m_e / m_h$.^{10,22} The plotted quantity in Fig. 7(a) is twice the difference of peak and half-height energies on the low-energy side. As a function of temperature, for the electron case there is an initial linear increase up to ~ 50

K, followed by a decrease to the empty-well value by ~ 150 K. At the same time, the oscillator strength decreases up to 80 K and then increases. With a hole sea the width is initially temperature independent, and then falls to the empty-well value, while the oscillator strength increases uniformly.

We can account qualitatively for this as follows. The existence of a singularity at the Fermi edge depends on the sharpness of the Fermi surface relative to the binding energy of the "Mahan exciton." With increasing temperature the Fermi edge broadens and the many-body electron-hole correlation decreases.²⁴ At the same time,

the phase-space blocking which prevents formation of the atomic exciton becomes ineffective, so that with increasing temperature the "Mahan exciton" evolves into the atomic exciton, which shows little broadening at 100 K. This decrease in linewidth observed in both the electron- and hole-sea cases reflects the fact that in neither case is $k_F a_0$ large compared to unity, so that the many-body effects inherent in the "Mahan exciton" are fairly weak.

A more quantitative test is represented by the solid curves in Fig. 7(b), which are predictions of the "Stokes shift" based on the assumption that it consists of a sum of components due to well-width fluctuations and to the temperature dependence of the quasichemical potential. The former component is obtained from the data for the empty well at 0.30 V bias, while the latter is calculated assuming that the carrier density remains constant with temperature and that the PLE peak coincides with the quasichemical potential at a given temperature. The Fermi energies are taken as 6.3 meV at 1.50 V bias and 1.0 meV at -0.70 V bias.

The good agreement for the 1.5-V data where $E_F \gg k_B T$ at the lowest temperature tends to confirm the theoretical prediction that the peak enhancement of the oscillator strength occurs near the quasichemical potential,²⁴ as also found by Livescu *et al.*,²⁵ and that we indeed have fully developed "Mahan excitons" up to nearly 100 K. At -0.7 V the agreement is poor. This suggests that the many-body effects giving rise to formation of "Mahan excitons" are less important in the hole sea than in the electron case, so that the observed absorption peak does not represent a fully formed "Mahan exciton" even at low temperatures, and we are observing only the recovery of the atomic exciton as the degeneracy of the hole sea is diminished. The latter picture is consistent with the fact that the quenching of the $E1-H1$ peak at -1.0 V ($0.75 \times 10^{11} \text{ cm}^{-2}$ heavy holes) in Fig. 2 is more complete than at 1.0 V ($1.8 \times 10^{11} \text{ cm}^{-2}$ electrons); at 1.0 V there is a many-body enhancement of the oscillator strength that is not present at -1.0 V.

VI. LUMINESCENCE UP-CONVERSION AND MECHANISM OF CHARGE ACCUMULATION

To investigate the interwell charge transfer as a function of applied bias in more detail, we created electrons and holes at low temperature by selective excitation of the 10-nm and wider wells with photons of energy < 1.56 eV while monitoring the integrated $E1-H1$ luminescence of the 5-nm well at 1.59 eV. Incident power density was 1 W cm^{-2} . The results are shown in Fig. 8. The integrated intensity [Fig. 8(a)] shows a strong peak near 1.0 V and a smaller peak near -0.2 V. The integrated intensity varied linearly with excitation intensity between 10^{-2} and 10^3 W cm^{-2} . Since direct excitation of the 5-nm well requires photon energies greater than 1.58 eV (see Fig. 2), observation of low-temperature luminescence for excitation at much lower energies must result from carriers generated elsewhere in the structure and transferred into the 5-nm well when the bands are tilted under applied bias. Quantum efficiency for the up-conversion was 10^{-2} – 10^{-3} times that for direct photoexcitation of the 5-nm well.

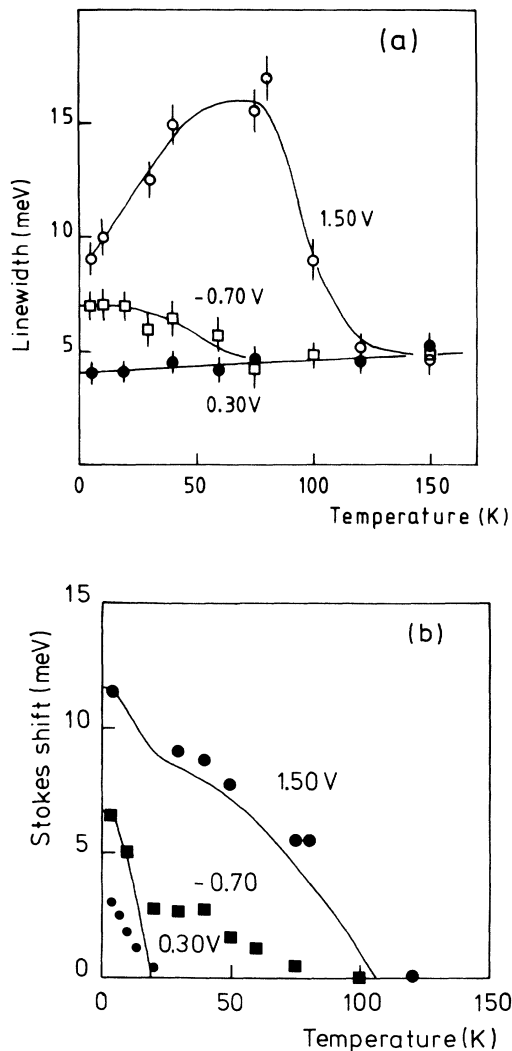


FIG. 7. (a) Temperature dependence of the $E1-H1$ photoluminescence excitation linewidth at the indicated biases, and (b) temperature variation of the "Stokes shift" between emission and absorption for the $E1-H1$ transition in the 5-nm well at biases corresponding to flat band (0.30 V), an electron density of $\sim 1.8 \times 10^{11} \text{ cm}^{-2}$ (1.5 V), and a hole density of $\sim 0.75 \times 10^{11} \text{ cm}^{-2}$ (-0.70 V). The solid curves in (b) are calculations of the variation in "Stokes shift" as described in the text for 1.5 and -0.7 V.

The action spectrum for the upconverted luminescence at 0.7 V [Fig. 8(b)] shows a peak corresponding to the band-edge exciton in GaAs (~ 1.515 eV) and the $E1-H1$ and $E1-L1$ transitions in the 10-nm well (1.54–1.55 eV). A similar spectrum is found for a reverse bias of -0.50 V. It is interesting that no peaks corresponding to the 20-nm well are observed, possibly due to quenching of the oscillator strength by the electric field or by phase-space filling under applied bias.

It is clear that the accumulation of electrons and holes in the 5-nm well under applied bias must be due to transport of carriers photoexcited in the 80-nm-thick GaAs layer and, possibly, in the buffer layer. The small number of the other carrier type necessary for recombination is then injected from the ITO electrode. The fact that the carriers only accumulate over restricted ranges of applied bias, as demonstrated by the “Stokes shift” (Fig. 3), suggests that resonant transfer between the wells is important. This conclusion is strengthened by our measurements of exciton dephasing using resonant Rayleigh scattering.¹⁶

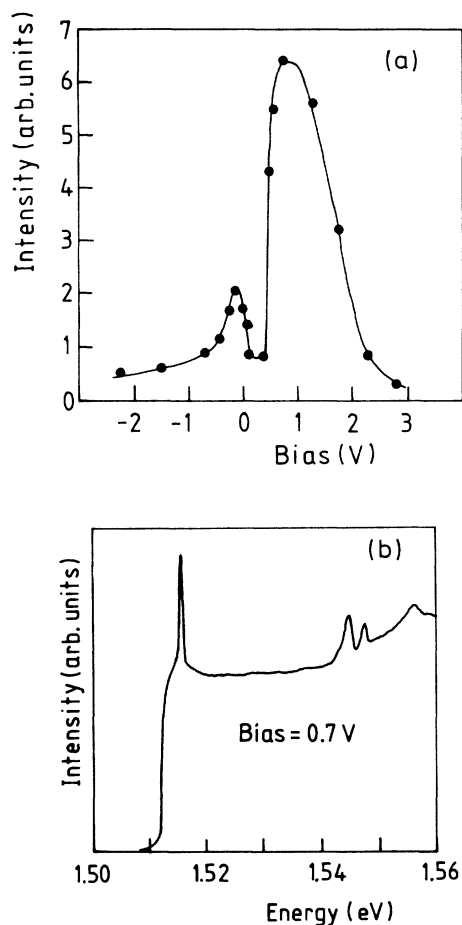


FIG. 8. (a) Integrated intensity of $E1-H1$ luminescence from the 5-nm well near 1.595 eV obtained by exciting the thicker wells in the structure at the lower energy of 1.547 eV. (b) Integrated luminescence intensity as in (a), but as a function of pumping energy at a fixed bias of 0.70 V.

We have not attempted a self-consistent calculation of the electric field distribution across the sample in the presence of charge accumulation. However, as the bands are tilted away from flat band under forward bias, it appears experimentally that electrons transfer into both the 5- and 10-nm-wide wells at approximately the same bias of 0.6 V. This is quite close to the bias required (0.70 V) to align the $n=1$ conduction subbands of the 20- and 10-nm wells, in the absence of charge accumulation, such that the voltage is dropped uniformly across the structure.

The 10-nm well is depopulated at an applied bias of about 1.0 V, which is approximately the bias required (1.25 V) to align the $n=1$ conduction-band states in the 5- and 10-nm wells. At 2.0 V the 5-nm well is depopulated. A similar chain of events takes place in reverse bias. There, the heavy-hole populations in the wells change dramatically at biases suggestive of the alignment of the light-hole bound states. Obviously, the detailed behavior is governed by a complicated interplay of transport and electrostatic effects which we have not modeled in detail, but the sharp onsets for filling and emptying of the wells are consistent with a transport mechanism dominated by tunneling of electrons in forward bias and light holes in reverse bias (which rapidly thermalize to heavy holes in the wells) and which requires the alignment of energy levels. The electrostatic effects of the charge transfer must cause very nonuniform internal field distributions and these may change rapidly with the transfer of small amounts of charge leading to a cooperative emptying or filling of wells.

The detailed mechanism of charge transport through thick barriers at low temperature is generally unclear. In our sample the dominant mechanism seems to be tunneling, possibly enhanced by defects (e.g., deep levels²⁶) within the barriers. At temperatures higher than 100–200 K thermal activation over the barriers generally provides a good picture of charge transport in GaAs/Ga_{1-x}Al_xAs multiple-quantum-well (MQW) structures with relatively thick barriers. In particular, efficient thermal activation explains the high quantum efficiency of pin MQW detectors when illuminated at energies below the barrier band gap. With decreasing temperature, the photocurrent in such structures has been observed to decrease, as expected for thermally activated transport, but saturates and sometimes increases²⁷ below 100 K, indicating the importance of tunneling at low temperatures.

It is interesting to compare the up-conversion phenomenon we have described with the charge or exciton transfer observed by Wilson *et al.*²⁸ in a similar GaAs/Al_xGa_{1-x}As structure to ours. These authors observed strong excitonic features in the PLE spectrum of a 10-nm well corresponding to transitions in an adjacent 5-nm well separated by a 30-nm Al_{0.37}Ga_{0.63}As barrier. They attributed this effect to exciton migration between the wells, possibly along dislocation chains, rather than to single-step tunneling of the kind discussed by Nelson *et al.*²⁹ Another possibility is that they were observing uncorrelated electron and hole migration. These measurements were made without externally applied field, al-

though there would have been a built-in field due to surface pinning of the Fermi level near midgap. In contrast to these results, we were unable to observe evidence of exciton features corresponding to thinner wells in the PLE spectra of thicker wells at any biases in our samples. This is consistent with the low up-conversion efficiency which we observe.

VII. SUMMARY

We have described a study of optical properties of the same quantum well over a range of carrier concentrations from $1.8 \times 10^{11} \text{ cm}^{-2}$ electrons through empty to $0.75 \times 10^{11} \text{ cm}^{-2}$ holes. This was made possible by use of a sample containing several quantum wells of different thicknesses separated by thick, though leaky, barriers. Carriers accumulate in the wells over restricted ranges of applied forward and reverse bias as a result of quasiresonant transfer of carriers photoexcited elsewhere in the structure. An important consequence of this is that it enables the carrier density and type in the wells to be varied merely by changing the bias, and thereby avoids the variations of parameters inherent in previous comparisons of different samples.

In particular, we have investigated the changeover from "atomic" to "Mahan" exciton behavior as a function of both carrier concentration and temperature, and have also measured the band-gap renormalization due to both electron and hole accumulation. We find a larger renormalization for a Fermi sea of holes than for electrons at the same sheet density. The atomic exciton is characterized by sharp bound states with relatively weak temperature dependence, whereas the "Mahan exciton" consists of a many-body enhancement of absorption near the Fermi energy, which is strong at low temperatures and rapidly disappears as the temperature approaches E_F/k_B . For the modest carrier concentrations available in this sample, the "Mahan exciton" evolves continuously into an atomic exciton as the temperature is increased further.

ACKNOWLEDGMENTS

The authors are grateful to W. M. Stobbs for confirmation of layer thicknesses by TEM. This work was partly supported by the United Kingdom Department of Trade and Industry Joint Opto-Electronic Research Scheme on Digital Optics and Computing.

*Present address: Max-Planck-Institut für Festkörperforschung, Heisenbergstrasse 1, Postfach 800665, D-7000 Stuttgart 80, West Germany.

†Present address: Department of Physics, The University of Southampton, Southampton SO9 5NH, Hampshire, United Kingdom.

¹R. Sooryakumar, D. S. Chemla, A. Pinczuk, A. C. Gossard, W. Wiegmann, and L. J. Sham, *Solid State Commun.* **54**, 859 (1985).

²A. E. Ruckenstein, S. Schmitt-Rink, and R. C. Miller, *Phys. Rev. Lett.* **56**, 504 (1986).

³C. Delalande, G. Bastard, J. Organasi, J. A. Brum, H. W. Lui, M. Voos, G. Weimann, and W. Schlapp, *Phys. Rev. Lett.* **59**, 2690 (1987).

⁴D. A. Kleinman and R. C. Miller, *Phys. Rev. B* **32**, 2266 (1985).

⁵D. Huang, H. Y. Chu, Y. C. Chang, R. Houdré, and H. Morçoç, *Phys. Rev. B* **38**, 1246 (1988).

⁶F. Stern and W. E. Howard, *Phys. Rev.* **163**, 816 (1967).

⁷S. Schmitt-Rink and C. Ell, *J. Lumin.* **30**, 585 (1985).

⁸A. E. Ruckenstein and S. Schmitt-Rink, *Phys. Rev. B* **35**, 7551 (1987).

⁹G. D. Mahan, *Phys. Rev.* **153**, 882 (1967).

¹⁰S. Schmitt-Rink, D. S. Chemla, and D. A. B. Miller, *Phys. Rev. B* **32**, 6601 (1985).

¹¹G. D. Mahan, *Phys. Rev.* **163**, 612 (1967).

¹²P. Nozières and C. T. de Dominicis, *Phys. Rev.* **178**, 1097 (1969).

¹³A. Pinczuk, J. Shah, R. C. Miller, A. C. Gossard, and W. Wiegmann, *Solid State Commun.* **50**, 735 (1984).

¹⁴M. S. Skolnick, J. M. Rorison, K. J. Nash, D. J. Mowbray, P. R. Tapster, S. J. Bass, and A. D. Pitt, *Phys. Rev. Lett.* **58**,

2130 (1987).

¹⁵A. S. Plaut, R. T. Harley, S. R. Andrews, and T. M. Kerr (unpublished).

¹⁶S. R. Andrews and R. T. Harley, *Proc. SPIE* **792**, 141 (1987); S. R. Andrews, R. T. Harley, and T. M. Kerr (unpublished).

¹⁷D. A. B. Miller, J. S. Weiner, and D. S. Chemla *IEEE J. Quantum Electron.* **QE-22**, 1816 (1986).

¹⁸E. Burstein, *Phys. Rev.* **93**, 632 (1954).

¹⁹A. S. Plaut, J. Singleton, R. J. Nicholas, R. T. Harley, S. R. Andrews, and C. T. B. Foxon, *Phys. Rev. B* **38**, 1323 (1988).

²⁰H. J. Pollard, L. Schultheis, J. Kuhl, E. O. Göbel, and C. W. Tu, *Phys. Rev. Lett.* **55**, 2610 (1985).

²¹D. A. Kleinman, *Phys. Rev. B* **32**, 3766 (1985).

²²J. Gavoret, P. Nozières, B. Roulet, and M. Combescot, *J. Phys. (Paris)* **30**, 987 (1969).

²³L. Schultheis, A. Honold, J. Kuhl, K. Köhle, and C. W. Tu, *Phys. Rev. B* **34**, 9027 (1986).

²⁴S. Schmitt-Rink, C. Ell, and H. Haug, *Phys. Rev. B* **33**, 1183 (1986).

²⁵G. Livescu, D. A. B. Miller, and D. S. Chemla, *Superlatt. Microstruct.* **4**, 359 (1988).

²⁶F. Capasso, K. Mohammed, and A. Y. Cho, *Phys. Rev. Lett.* **57**, 2303 (1986).

²⁷R. T. Collins, K. v. Klitzing, and K. Ploog, *Appl. Phys. Lett.* **49**, 406 (1986).

²⁸B. A. Wilson, R. C. Miller, S. K. Spitz, H. D. Harris, R. Sauer, M. G. Lamont, C. W. Tu, and R. F. Kopf, in *Gallium Arsenide and Related Compounds*, Inst. Phys. Conf. Ser. No. 83, edited by W. T. Lindley (IOP, Bristol, 1987), p. 215.

²⁹D. F. Nelson, R. C. Miller, D. A. Kleinman, and A. C. Gossard, *Phys. Rev. B* **34**, 8671 (1986).